FEMS Microbiology Letters, 368, 2021, fnab002

doi: 10.1093/femsle/fnab002
Advance Access Publication Date: 8 January 2021
Research Letter

RESEARCH LETTER – Environmental Microbiology

The starlet sea anemone, *Nematostella vectensis*, possesses body region-specific bacterial associations with spirochetes dominating the capitulum

Anthony M. Bonacolta[1,†], Michael T. Connelly[1,‡], Stephanie M. Rosales[2,3], Javier del Campo[1] and Nikki Traylor-Knowles[1,*,#]

[1]Department of Marine Biology and Ecology, Rosenstiel School of Marine and Atmospheric Science, University of Miami, 4600 Rickenbacker Causeway, Miami, FL 33149, USA, [2]Atlantic Oceanographic and Meteorological Laboratory, National Oceanic and Atmospheric Administration, Miami, FL 33149, USA and [3]Cooperative Institute for Marine and Atmospheric Studies, University of Miami, Miami, FL 33149, USA

*Corresponding author: Rosenstiel School of Marine and Atmospheric Science University of Miami, 4600 Rickenbacker Causeway, Miami, FL 33149, USA. Tel: 305-421-4394; E-mail: ngt14@miami.edu

One sentence summary: A significant capitulum-specific dominance of spirochetes within *Nematostella vectensis* was revealed through an original, body-region microhabitat sampling design.

Editor: Yu-Zhong Zhang
†Anthony M. Bonacolta, http://orcid.org/0000-0003-1439-5907
‡Michael T. Connelly, http://orcid.org/0000-0002-2084-4222
#Nikki Traylor-Knowles, http://orcid.org/0000-0002-4906-4537

ABSTRACT

Sampling of different body regions can reveal highly specialized bacterial associations within the holobiont and facilitate identification of core microbial symbionts that would otherwise be overlooked by bulk sampling methods. Here, we characterized compartment-specific associations present within the model cnidarian *Nematostella vectensis* by dividing its morphology into three distinct microhabitats. This sampling design allowed us to uncover a capitulum-specific dominance of spirochetes within *N. vectensis*. Bacteria from the family Spirochaetaceae made up 66% of the community in the capitulum, while only representing 1.2% and 0.1% of the communities in the mesenteries and physa, respectively. A phylogenetic analysis of the predominant spirochete sequence recovered from *N. vectensis* showed a close relation to spirochetes previously recovered from wild *N. vectensis*. These sequences clustered closer to the recently described genus *Oceanispirochaeta*, rather than *Spirochaeta perfilievii*, supporting them as members of this clade. This suggests a prevalent and yet uncharacterized association between *N. vectensis* and spirochetes from the order Spirochaetales.

Keywords: spirochetes; cnidarian; *Nematostella vectensis*; microbiome; 16S rRNA; anemone

INTRODUCTION

The discovery of microhabitat-specific microbial communities has become important for our understanding of microbial interactions and diversity (Ainsworth, Thurber and Gates 2010; Bourne, Morrow and Webster 2016). For example, in the giant clam, *Tridacna maxima*, different tissues harbor distinct microbial communities, with the gills harboring a high prevalence of *Endozoicomonas* bacteria (Rossbach 2019). Evaluation of the discrete tissues of *T. maxima* helped uncover *Endozoicomonas*'s role

Received: 24 August 2020; **Accepted:** 6 January 2021

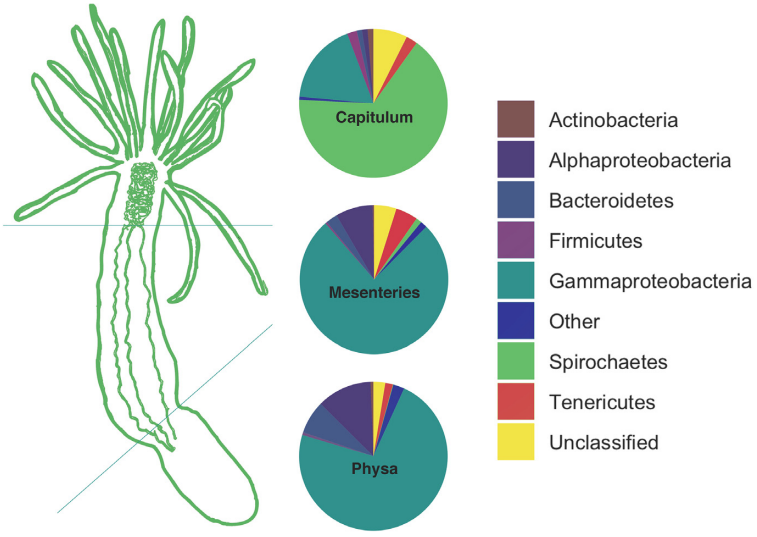

Figure 1. Compartmentalization of the microbiome in *N. vectensis*. The microbiome of *N. vectensis* was divided into three tissue compartments for this study: the capitulum, mesenteries and physa. The capitulum had a bacterial community dominated by Spirochaetes. The mesenteries and physa had a bacterial community dominated by Gammaproteobacteria and Alphaproteobacteria, with very little presence of Spirochaetes.

in nitrogen cycling within the holobiont (Rossbach 2019). The microhabitats within animal tissues are proposed to strongly influence the composition of the microbial community (Vaishnava *et al.* 2008; Hooper, Littman and Macpherson 2012). Consequently, the specific composition of each microhabitat can provide clues as to the community's functional contribution to host physiology (Ainsworth, Thurber and Gates 2010).

In the phylum Cnidaria (sea anemones, corals, etc.), many species are known to associate with different microbial partners, including bacteria, and these relationships are known to be important for the cnidarian host health (Rädecker *et al.* 2015; Bourne, Morrow and Webster 2016; Robbins *et al.* 2019). For instance, in the red coral *Corallium rubrum*, spirochetes are known to dominate the bacterial community and have a potential role in the nitrogen cycle of the holobiont (van de Water *et al.* 2016). Previous studies have found that sampling methods can bias microbiome composition by only sampling certain regions of the organism, such as the mucus, skeleton or tissue (Sweet, Croquer and Bythell 2011). On the other hand, agglomerated samples of all these microhabitats can mask potentially important associations. An advantage of microhabitat sampling of an organism's body is that it can facilitate the identification of core microbial symbionts in different body microhabitats, which likely represent highly specialized symbiotic associations (Apprill, Weber and Santoro 2016; Bourne, Morrow and Webster 2016). However, in the model sea anemone, *Nematostella vectensis*, the presence of body region-specific microhabitats of bacterial communities has not previously been identified.

Nematostella vectensis is an estuarine sea anemone found in salt marshes along both the Atlantic and Pacific coastlines of North America (Hand and Uhlinger 1994). It has rapidly gained popularity as a model organism because it is easy to rear in the lab, simple to manipulate and has a wide range of available genomic resources (Putnam *et al.* 2007; Reitzel, Ryan and Tarrant 2012). *Nematostella vectensis* is diploblastic and possesses a mouth surrounded by 12–16 tentacles (Renfer *et al.* 2010). It has a clearly defined pharynx and mesenteries that run along the oral–aboral axis and a physa at the aboral end used for digging (Layden *et al.* 2010). The sequencing of the *N. vectensis* 16S ribosomal RNA (rRNA) microbiome has increased our understanding of the microbial community diversity that is crucial for understanding nutrient cycling, defense against diseases, thermoregulation and the ability to rapidly adapt to environmental stressors (Rosenberg *et al.* 2007; Mortzfeld *et al.* 2016). Previous studies using 16S rRNA gene sequencing, gene expression analysis and whole-genome sequencing to compare wild and lab-reared *N. vectensis* found that they are primarily associated with the bacteria phyla: Bacteroides, Chloroflexi, Cyanobacteria, Firmicutes, Proteobacteria and Spirochaetes (Har *et al.* 2015). Other studies on the *N. vectensis* microbiome have found that it is diverse in anemones cultured in constant darkness and that it is heavily influenced by developmental stage (Mortzfeld *et al.* 2016; Domin *et al.* 2018; Leach, Carrier and Reitzel 2019). Although the microbiome was more diverse in dark conditions, it is still represented by a 'core' microbiome of the same phyla noted above (Leach, Carrier and Reitzel 2019). The current information on *N. vectensis* suggests that the microbiome is a highly dynamic and complex community that responds to environmental cues. However, these patterns were observed in the whole organism, which may obscure important niche-specific bacteria compartments within *N. vectensis*.

In this study, we will distinguish the bacterial microbiomes of the three *N. vectensis* body compartments: the capitulum (pharynx + tentacles), mesenteries and physa by using 16S rRNA gene amplicon sequencing (Fig. 1). Previous studies have used this similar division of *N. vectensis* body regions (Zenkert *et al.* 2011; Stefanik, Friedman and Finnerty 2013). Note that these three microhabitats are only body-regionally descriptive, meaning each sample type includes all tissue layers of that region (i.e. endodermis and epidermis). We hypothesized that different body regions or 'microhabitats' of *N. vectensis* possess distinguishable microbiomes, potentially revealing specialized partnerships previously overlooked by whole-organism sampling. We found that the capitulum possesses significantly different bacterial community abundances compared with the mesenteries and physa and that spirochetes are the dominant bacterial phylum present in the capitulum. Spirochetes were previously identified in *N. vectensis*; however, their specific microhabitat was unknown. This study will better clarify our understanding of the bacterial community diversity in *N. vectensis* and shed

light on the importance of microhabitat sampling in microbiome studies.

METHODS

Nematostella vectensis culture and care

The individuals used for this study are lab-cultured animals that have been housed at the Rosenstiel School of Marine and Atmospheric Science (RSMAS) Cnidarian Immunity Lab since 2016. Lab-cultured animals were used in this study in order to minimize potential collection site-specific environmental variables, such as water pH, tidal cycles and anthropogenic activity/pollution on the microbiome. All animals were kept in the dark at room temperature (~23.8°C) within covered glass dishes filled with 11 parts per thousand 2-μm filtered seawater (FSW). Two months prior to the beginning of this study, *N. vectensis* adults were placed into a single glass dish and fed mussels three days a week, and *Artemia* five days a week for two months in order to increase their size (Stefanik, Friedman and Finnerty 2013). Water changes were conducted an hour after each mussel feeding. One week before beginning the trisection (see the next section), the largest individuals were transferred individually into a 12-well plate with sterilized FSW and starved for seven days to minimize microbial carryover from food. Previous studies found that a two-day starving period was sufficient to eliminate digested food and potential food contamination; however, for extra caution, we increased our starvation time to seven days (Har *et al.* 2015; Leach, Carrier and Reitzel 2019). We selected the largest individuals to maximize the precision of our trisection cuts and the amount of tissue we could get from each individual in this way. The sex of the anemones was not determined; in other cnidarians, sex was determined to have a minor effect on the microbiome composition and therefore was not included in this study (Wessels *et al.* 2017).

Trisection

Six adult *N. vectensis* were anesthetized using 7% $MgCl_2$ solution, washed with sterilized FSW and then aseptically trisected. $MgCl_2$ solution has been shown to disrupt the mucus of the ectodermal layer in cnidarians, so the mucus microbiome was likely affected by this treatment. The trisection resulted in the isolation of three tissue compartments from each anemone: (i) capitulum (pharynx and tentacles), (ii) mesenteries and (iii) physa (Fig. 1). These body regions were chosen because they were easily distinguishable and represented different functional regions of the organism. The scalpel and tweezers were flame and ethanol sterilized between tissue dissections. Care was made to cut as cleanly as possible to limit any cross-contamination of tissue compartments. The cut for the capitulum and mesentery boundary was established as just below the visible pharynx. Some physa tissue was found in the mesentery compartment as the mesenteries were not directly removed from the body cavity. However, the physa compartment did not contain any mesentery material. Each sample was then stored in a 2-mL centrifuge tube with RNAlater (Sigma Aldrich, St Louis, MO) and placed in a −80°C freezer. In total, there were 18 samples ($n = 6$ capitulum, $n = 6$ mesenteries and $n = 6$ physa) that were further processed.

16S rRNA PCR and sequence library preparation

Total DNA was extracted from all samples using the Qiagen DNeasy Powersoil Kit (Qiagen, Hilden, Germany). The concentration and quality of the DNA were assessed using a NanoDrop spectrophotometer (Thermo Fisher Scientific Inc., Waltham, MA). The DNA was then stored in a −80°C freezer until library preparation. High-throughput 16S rRNA amplicon sequencing methods were adapted from the protocol developed by the Earth Microbiome Project (Thompson *et al.* 2017). In short, the V4 region of the 16S rRNA gene [515F (5′-GTGCCAGCMGCCGCGGTAA-3′)–806R (5′-GGACTACHVHHHTWTCTAAT-3′) primers] was amplified using polymerase chain reaction (PCR) on 18 tissue samples (Apprill *et al.* 2015). A negative non-template control was also amplified to account for extraction and PCR contamination. A total of 50 μL of PCR reaction mixtures was prepared according to the following recipe: 23 μL PCR-grade water, 20 μL PCR master mix (2×), 1 μL 806R primer (10 μM), 1 μL barcoded 515F primer (10 μM) and 5 μL template DNA. The PCR was performed with the following program: 1 × 3 min at 94°C, 35 × (45 s at 94°C, 60 s at 50°C, 90 s at 72°C) and 1 × 10 min at 72°C. The PCR products were run on a 1.5% agarose gel to check for correct amplification size. Following the gel electrophoresis, PCR products were cleaned using AMPure XP Beads (Beckman Coulter Inc., Brea, CA). DNA concentrations were quantified using the Qubit dsDNA high sensitivity (HS) kit (Thermo Fisher Scientific Inc., Waltham, MA) and samples were diluted to 4 nM using PCR-grade water. Five microliters of each sample was then pooled into a single 1.5-mL tube. The pooled PCR products were then sequenced on an Illumina MiSeq PE300 sequencer at the Center for Genome Technology at the University of Miami's Miller School of Medicine. Raw Illumina paired-end reads have been deposited in the NCBI Sequence Read Archive database under BioProject PRJNA610635.

Post-sequencing processing and statistical analysis

Post-sequencing processing was conducted using the Quantitative Insights in Microbial Ecology 2 (QIIME2) v2019.1 pipeline (Bolyen *et al.* 2019). Demultiplexed paired-end reads were then merged using DADA2 v1.10.0 and to yield amplicon sequence variants (ASVs) (Callahan *et al.* 2016). Within the DADA2 pipeline, the forward sequences were truncated at 200 bp and reverse sequences were truncated at 180 bp, and then sequences found to be chimeric were removed using the 'consensus' method option within the program. Taxonomy was then assigned to our sequences using the SILVA 132 99% classifier (https://data.qiime2.org/2019.10/common/silva-132-99-nb-classifier.qza) (Quast *et al.* 2013). Mitochondria and chloroplast sequences were then filtered from the feature table in order to remove any eukaryotic-derived 16S rRNA gene sequences. The QIMME2 output was then transferred to R and further analysis and processing were done using the phyloseq R package v1.28.0 (McMurdie and Holmes 2013). Microbial contaminants were then removed using decontam v1.4.0 (Davis *et al.* 2018). All sequences that were more prevalent in the negative control than in the samples were removed. We then used DESeq2 v1.24.0 to normalize our dataset using a variance stabilizing transformation (VST) (Love, Huber and Anders 2014). To account for abundance and evenness of microbial taxa within the VST dataset, the Shannon–Weiner diversity index and Simpson's diversity index were calculated for each compartment region using phyloseq. The Shannon–Weiner diversity index is the most commonly reported alpha-diversity metric in microbiome studies (followed by general species richness) and is thought to be the most robust and informative (Haegeman *et al.* 2013; Reese and Dunn 2018). Both the Shannon–Weiner diversity index and

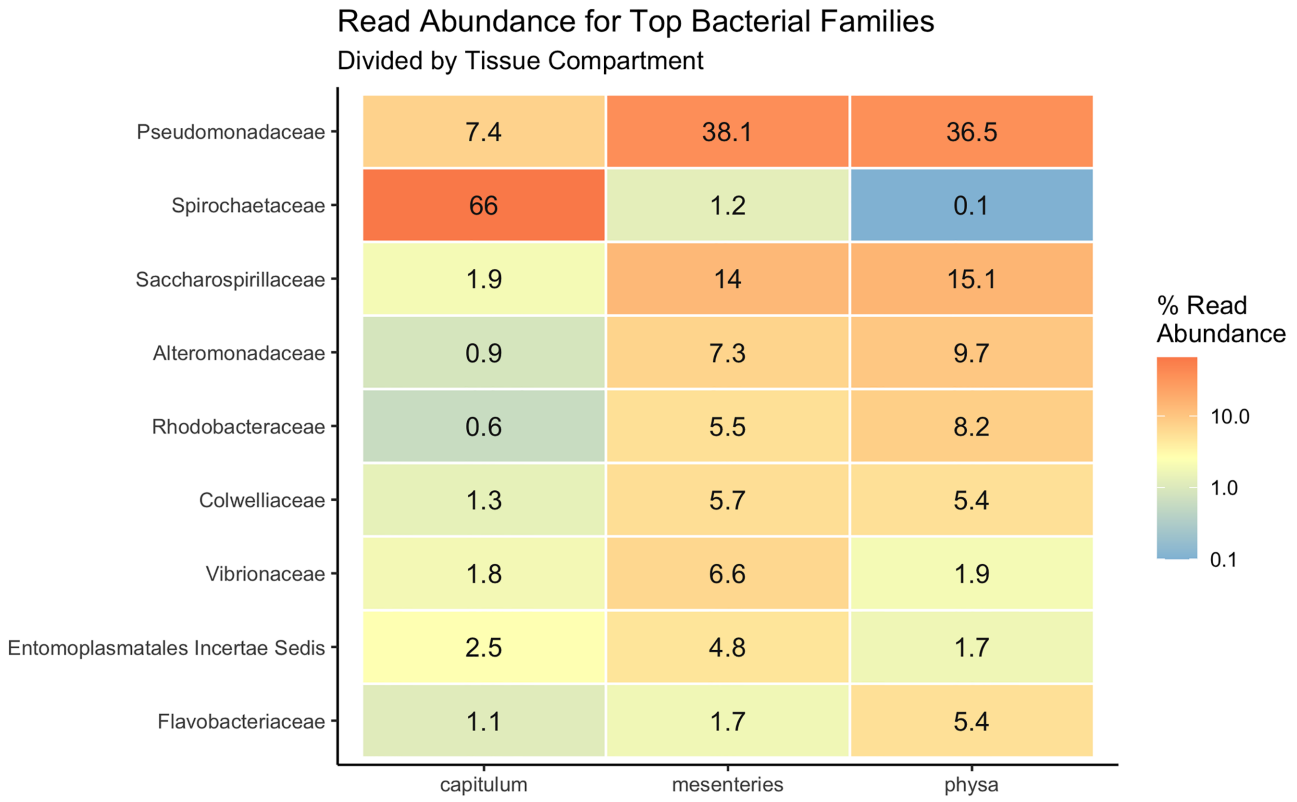

Figure 2. Heat map of the % read abundance for top bacterial families found in *N. vectensis* separated by tissue compartment. Bacteria of the family Pseudomonadaceae were found to be the most prevalent in the mesentery and physa tissues of *N. vectensis* (38.1% and 36.5% abundance, respectively). In contrast, Pseudomonadaceae only had a 7.4% abundance in capitulum tissue. Likewise, Spirochaetaceae were found to make up 66% of the community within the capitulum tissue of *N. vectensis*, while only being 1.2% and 0.1% abundant in the mesentery and physa tissues, respectively. Overall, the capitulum tissue appears to have a very distinct community from the mesenteries and physa.

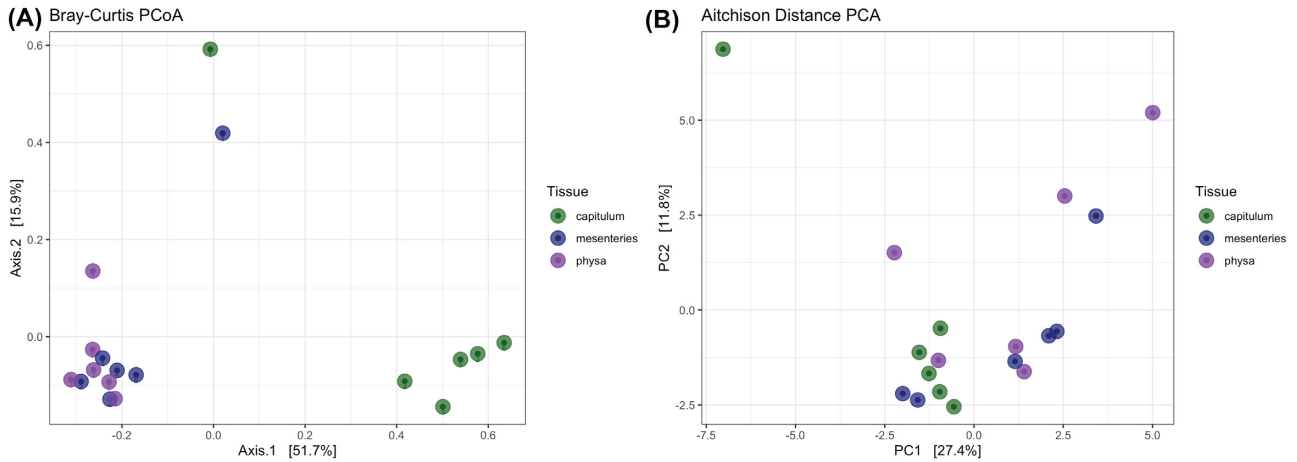

Figure 3. Beta-diversity measures between tissue regions of *N. vectensis*. **(A)** Bray–Curtis principal coordinate analysis of *N. vectensis* bacterial communities after a variance-stabilizing transformation. Capitulum samples clustered tightly, while physa and mesentery communities clustered closely together. **(B)** Aitchison principal component analysis (Euclidean distance of centered log-ratio transformed sample counts) of *N. vectensis* bacterial communities. Again, most capitulum samples clustered closely together; however, they were also clustered with mesenteries and physa samples.

the Simpson's diversity index have been recommended over general species richness when comparing microbiome diversity (Haegeman *et al.* 2013). We opted to include all three alpha-diversity metrics to enable better comparison to past and future studies. DESeq2 v1.24.0 and the QIIME2 add-on, analysis of composition of microbiomes (ANCOM), were used for microbial differential abundance analysis against tissue compartments and differences were considered significant if they had a *P*-value < 0.05. Random forest classifier modeling was performed using randomForest in order to determine the main bacterial taxa driving tissue compartment composition (Liaw and Wiener 2002). To visualize the most abundant bacterial families according to tissue compartment, heat maps were generated using the Ampvis2 v2.5.7 (Andersen *et al.* 2018).

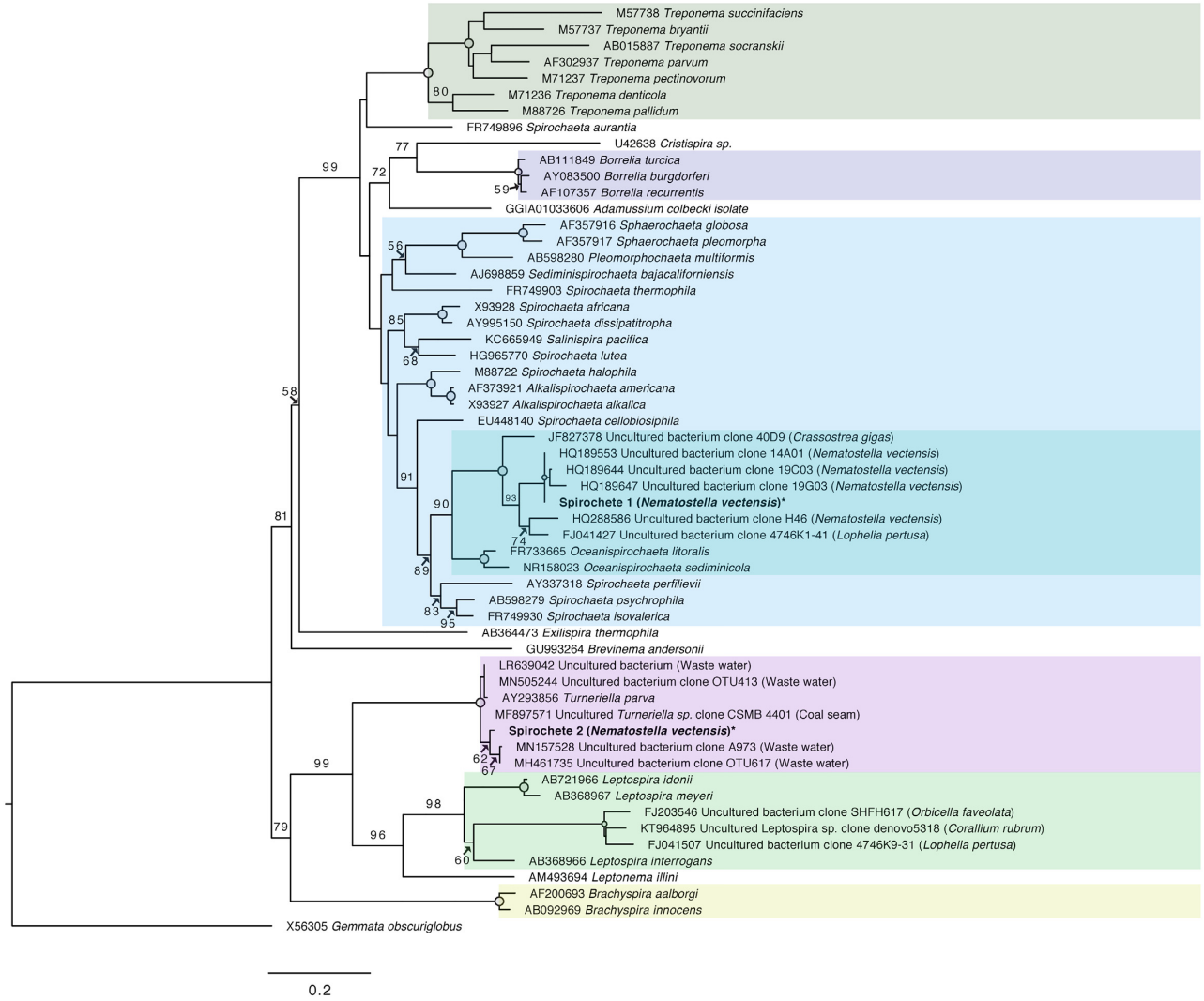

Figure 4. Best-fit maximum likelihood tree based on 16S rRNA sequences depicting the phylogenetic relationship of the spirochetes recovered from the capitulum of *N. vectensis*. This tree was constructed using RAxML v7.3.0 with 1000 sub-samplings. Bootstrap values (>50%) are shown. Nodes with 100% bootstrap support are indicated by open circles. GenBank accession numbers are listed before the name of each sequence. The host/habitat of uncultured species is in parentheses. Spirochetes from this study are in bold. Shading corresponds to major clades within the phylum Spirochaetae. *Gemmata obscuriglobus* was used as an outgroup to root the tree. The predominant spirochete ASV from this study (Spirochete 1) forms a strongly supported (100% bootstrap) monophyletic clade with spirochete sequences recovered from wild *N. vectensis*. Spirochete 2 clusters within the genus *Turneriella*.

For beta-diversity measurements, both Bray–Curtis and Aitchison (Euclidean distances of centered log-ratio transformed counts) distance matrices were assessed as both are commonly used in microbial community studies. Here, we included both analyses to allow for comparisons to previous studies (Mortzfeld *et al.* 2016; Domin *et al.* 2018). Following recommended methods, the VST-transformed data were used to calculate the Bray–Curtis distances, while the Aitchison distances were calculated on the centered log-ratio transformation of the raw count data using the R package Microbiome v1.6.0 (Lahti and Shetty 2018). The program Vegan v2.5.6 was used to calculate Bray–Curtis and Euclidean distances. Within Vegan v2.5.6, the *Adonis* function was used to perform Permutational multivariate analysis of variance (PERMANOVA) analyses in order to statistically assess dissimilarity in microbial community composition between tissue compartments (Oksanen *et al.* 2011). All associated codes can be found on GitHub (https://github.com/Abonacolta/Nvec_Microhabitats).

Mapping *N. vectensis* ASVs to a phylogenetic tree of spirochetes

To understand the phylogenetic placement of the *N. vectensis* spirochetes, we mined NCBI using BLASTn, collected spirochete ASVs from previously published environmental metabarcoding studies and identified representatives of all major spirochete lineages. We then produced a reference tree using a total of 56 sequences composed of representative spirochetes and those environmental sequences identified as possessing 97% similarity to the two *N. vectensis* spirochete ASVs recovered in this study (Table S1, Supporting Information). A planctomycete sequence was used as an outgroup, as it is from a relatively closely related taxon of aquatic bacteria. These sequences were aligned using automatic settings of the program MAFFT v7.450 with the L-INS-i strategy (Katoh and Standley 2013). The alignment was trimmed to remove columns with gaps in >70% of the sequences or with a similarity score below 0.001 using Tri-

mAl v1.2 (Capella-Gutiérrez, Silla-Martínez and Gabaldón 2009). Using this trimmed alignment, a maximum-likelihood tree was then constructed using RAxML v7.3.0 with the GTRCAT substitution model and 1000 sub-samplings to generate a best-fit tree (Stamatakis 2014). The final tree was visualized in FigTree v1.4.4 (Drummond *et al.* 2012).

RESULTS AND DISCUSSION

The body regions of *N. vectensis* exhibited distinct bacterial associations

An average of 117 606 ± 8293 reads per sample was generated and a total of 620 ASVs were determined. Five of the 620 ASVs were removed due to suspected contamination. We found that the microbial composition of the capitulum is distinct from the mesenteries and physa (Fig. 1). Overall, the microbiomes were consistent between samples of the same microhabitat; however, one individual harbored a different compartmental microbiome from the others in this study (Figures S1–S3, Supporting Information). Individual 1 had all three microhabitats dominated by Proteobacteria, with only the physa compartment showing resemblance to the other individuals (Figures S1 and S3, Supporting Information). While individual 1 may just be an outlier, it highlights the need for additional sampling to uncover the true variability between conspecific tissue compartments. The family Spirochaetaceae, predominantly one ASV, made up ∼66% of the bacterial community within the capitulum but only ∼1.2% and ∼0.1% of the community in the mesenteries and physa, respectively (Fig. 2). This finding is similar to the microbiome of the crown-of-thorns sea star, *Acanthaster planci*, which found a high relative abundance (43–64%) of spirochetes only within the body wall compartment (Høj *et al.* 2018). Prior to this, Alphaproteobacteria was thought to be the most abundant bacterial phylum across sea stars (Lawrence *et al.* 2010). Additionally, previous studies on the microbiome of developing *N. vectensis* found that as development progresses Betaproteobacteria, Actinobacteria and Bacteroidetes abundances decrease, while Spirochaetes abundances increase in the adult organism (Mortzfeld *et al.* 2016). The development and growth of the capitulum during this time span may explain the high relative abundance of spirochetes that we saw in the capitulum. Spirochetes may play an active role in the capitulum development of *N. vectensis* and their ability to establish dominance over the Proteobacteria present throughout the rest of *N. vectensis* implies a competitive advantage on the part of the spirochete. Environmental bacteria can induce development in a number of marine eukaryotes from green algae and choanoflagellates to cnidarians, poriferans and echinoderms (Woznica and King 2018). In cnidarians, some Gammaproteobacteria and Actinobacteria have been observed to induce larval metamorphosis in anthozoans and scyphozoans (Neumann 1979; Tebben *et al.* 2011). The potential molecular cues from the spirochetes of *N. vectensis* should be investigated further. Spirochetes can preferentially thrive over other microbes in a host microhabitat because of their unique motility suitable for host invasion and their ability to attach to eukaryotic cells with specialized cellular structures (Canale Parola 1977; Wolgemuth 2015). Of note is that spirochetes are not found in high abundance in *Artemia* or mussel, the two food sources for the *N. vectensis* used in this study (Quiroz *et al.* 2015; Weingarten, Atkinson and Jackson 2019).

Gammaproteobacteria had an ∼76.3% and ∼72.9% relative abundance in the mesenteries and physa of *N. vectensis*, respectively, compared with an ∼17.8% relative abundance found in the capitulum (Fig. 1; Figure S2, Supporting Information). Gammaproteobacteria have previously been hypothesized to be important for microbial community structuring in juvenile *N. vectensis* (Domin *et al.* 2018). In addition to the Gammaproteobacteria, the physa of *N. vectensis* was dominated by the classes Alphaproteobacteria and Bacteroidetes with relative abundances of ∼11.9% and ∼7.2%, respectively (Figure S2, Supporting Information). This is similar to previous microbiome studies on lab-reared *N. vectensis* (Har *et al.* 2015; Mortzfeld *et al.* 2016; Leach, Carrier and Reitzel 2019). These studies found that Proteobacteria, including the classes Gammaproteobacteria and Alphaproteobacteria, were the most abundant bacterial phyla, while other taxa including Firmicutes, Planctomycetes, Tenericutes, Verrucomicrobia and Spirochaetes had lower abundances (Har *et al.* 2015; Mortzfeld *et al.* 2016; Leach, Carrier and Reitzel 2019). The predominant Gammaproteobacteria in the mesenteries consisted of members of the orders Oceanospirillales and Pseudomonadales. Oceanospirillales had a relative abundance of ∼38.1% in this microhabitat, while Pseudomonadales had an ∼14.5% relative abundance (Figure S3, Supporting Information). Pseudomonadaceae had the highest relative abundance in both the mesenteries and physa with ∼36.5% and ∼38.1%, respectively (Fig. 2; Figure S3, Supporting Information). This result supports previous findings that found Proteobacteria and Pseudomonas occur predominantly in aggregates along the walls of the mesenteries (Har 2009).

Differential microbial community structure between body regions

The taxonomic make-up of the *N. vectensis* microbiome varied according to body region. Comparing the drivers of bacterial community differential abundance across tissue compartments using a random forest classifier showed that the phyla Lentisphaerae, Proteobacteria and Spirochaetes were the strongest predictors of tissue compartments. According to differential abundance analysis, Spirochaetes and Fusobacteria were significantly more abundant in the capitulum compared with the other compartments (DESeq2; P-adj = 0.0000 and 0.0003, respectively). Lentisphaerae, Proteobacteria and Chloroflexi were more abundant in the mesenteries compared with the capitulum (DESeq2; P-adj = 0.0000, 0.0058 and 0.0009, respectively). Differential abundance analysis using ANCOM found that Spirochaetes and Bacteroidetes were the most differentially abundant phyla among tissue compartments (ANCOM; $W = 16$ and 14, respectively). Comparing the findings from both programs, Spirochaetes were the only taxon to be considered significantly differentially abundant or a predictor of body region in *N. vectensis* (Figure S4, Supporting Information). The body compartments of *N. vectensis* sampled in this study exhibited discrete microbial community structures. Alpha-diversity metrics showed a significant difference in the biodiversity and species richness present in different tissue compartments. Species richness between the capitulum and the mesenteries and physa was significantly different (ANOVA; $P = 0.023$ and 0.033, respectively; Figure S5, Supporting Information). The Simpson's index between the capitulum and the mesenteries and physa was also significantly different (ANOVA; $P = 0.039$ and 0.022, respectively; Figure S5, Supporting Information). However, the Shannon's diversity index did not show a significant difference in alpha diversity among body regions (ANOVA; $P = 0.11$ and 0.069, respectively; Figure S5, Supporting Information). Overall, all three alpha-diversity metrics showed a similar trend. Consistently, the capitulum of *N. vectensis* showed lower species richness compared with the mesenteries and physa. A similar

pattern was identified in the Simpson's index, with the capitulum showing a lower species diversity, but with a higher variation between individuals. We hypothesize that the lower species richness in the capitulum was likely driven by the dominance of the one single Spirochete ASV. In the future tests, using specific primers targeting this Spirochete ASV would be valuable to confirm this hypothesis.

Both Bray–Curtis dissimilarity and Aitchison distance were used to assess the differences in the microbial communities between tissue compartments (Fig. 3). A multivariate homogeneity of group dispersion analysis confirmed that an ANOVA test could appropriately be performed on both datasets (Koleff, Gaston and Lennon 2003). Bacterial communities between tissue compartments showed significant dissimilarity (PERMANOVA; permutations = 9999, $P = 0.0315$) according to the Bray–Curtis dissimilarity index. However, the same PERMANOVA test on the Aitchison distances found insignificant dissimilarity between tissue compartments (PERMANOVA; permutations = 9999, $P = 0.3294$). Aitchison distances account for the compositional nature of sequencing datasets and have recently been considered the new standard in the field (Quinn *et al.* 2018). Bray–Curtis distances have traditionally been used in microbiome studies, so we opted to include this analysis as well for comparison with previous work. More sampling is likely necessary to determine whether there is significant dissimilarity between the *N. vectensis* microhabitats sampled here. Of note is that even though no significant dissimilarity was found in the overall microbial composition of the microhabitats sampled, microhabitat-specific abundance patterns were still uncovered using this sampling strategy.

Phylogenetic analysis of *N. vectensis* spirochetes

The majority of spirochetes found in the capitulum were from a single ASV (Spirochete 1) within the order Spirochaetales. In order to better understand the phylogenetic placement of the spirochetes within *N. vectensis*, we conducted a phylogenetic analysis of this ASV along with the other spirochete ASV (Spirochete 2) recovered in this study (Fig. 4). Ninety three percent bootstrap support placed Spirochete 1 as closely related to four spirochete ASVs previously recovered from wild *N. vectensis* supporting the hypothesis that this spirochete is a consistent associate of the anemone (Har *et al.* 2015; Fig. 4). The *N. vectensis* spirochete ASVs also showed a strong relation to a spirochete recovered from the cold-water coral, *Lophelia pertusa*. Together, these sequences formed a 90% bootstrap-supported monophyletic clade with the two representative species of the recently described genus *Oceanispirocheata*. The genus *Oceanispirochaeta* consists solely of two representatives, *O. litoralis* and *O. sediminicola*, which are Gram-negative, moderately halophilic and obligately anaerobic (Subhash and Lee 2017).

One hundred percent bootstrap support was found for a node with Spirochete 2, several closely clustering wastewater ASVs and *Turneriella parva*, which is a Gram-negative, obligately aerobic spirochete with morphological similarities to *Leptospira* (Stackebrandt *et al.* 2013). This indicates that Spirochete 2 is unique from Spirochete 1 in species and potential function. Spirochetes associated with a diverse group of corals, including *C. rubrum*, *Orbicella faveolata* and *L. pertusa*, did form a 100% bootstrap monophyletic clade within the genus *Leptospira*, despite the broad geographical ranges of these coral species (*O. faveolata* is a Caribbean species, *C. rubrum* is a Mediterranean species and *L. pertusa* is a deep-sea species) indicating a potentially conserved association of these bacteria with cnidarians.

CONCLUSION

In this study, we characterized the microbiome of three distinct microhabitats within *N. vectensis*. A capitulum-specific dominance of spirochetes was uncovered highlighting the possible importance of these bacteria for *N. vectensis* physiology. Previous bulk-sampling techniques could not untangle these body compartment-specific bacterial associations, which should be taken into consideration in future cnidarian studies. Specifically, the role of spirochetes within the capitulum of *N. vectensis* should be further considered in subsequent studies. Overall, our findings provide support for spirochete as a consistent bacterium associated within *N. vectensis* and suggest that the functional role of this bacterium in the capitulum may be important for the anemone.

ACKNOWLEDGMENT

The authors would like to thank members of the Cnidarian Immunity Lab for comments and suggestions as this project was developing.

SUPPLEMENTARY DATA

Supplementary data are available at *FEMSLE* online.

FUNDING

AMB was supported by the Rosenstiel School of Marine and Atmospheric Science Small Undergraduate Research Grant Experience (SURGE) Award. NTK was supported by start-up funds from the Rosenstiel School of Marine and Atmospheric Sciences of the University of Miami, and by the National Science Foundation Award No. 1951826.

Conflict of Interest. None declared.

REFERENCES

Ainsworth TD, Thurber RV, Gates RD. The future of coral reefs: a microbial perspective. *Trends Ecol Evol* 2010;**25**:233–40.

Andersen K, Kirkegaard R, Karst S *et al.* ampvis2: an R package to analyse and visualise 16S rRNA amplicon data. *bioRxiv* 2018:299537.

Apprill A, McNally S, Parsons R *et al.* Minor revision to V4 region SSU rRNA 806R gene primer greatly increases detection of SAR11 bacterioplankton. *Aquat Microb Ecol* 2015;**75**:129–37.

Apprill A, Weber LG, Santoro AE. Distinguishing between microbial habitats unravels ecological complexity in coral microbiomes. *mSystems* 2016;**1**:e00143–16.

Bolyen E, Rideout JR, Dillon MR *et al.* Reproducible, interactive, scalable and extensible microbiome data science using QIIME 2. *Nat Biotechnol* 2019;**37**:852–7.

Bourne DG, Morrow KM, Webster NS. Insights into the coral microbiome: underpinning the health and resilience of reef ecosystems. *Annu Rev Microbiol* 2016;**70**:317–40.

Callahan BJ, McMurdie PJ, Rosen MJ *et al.* DADA2: high-resolution sample inference from Illumina amplicon data. *Nat Methods* 2016;**13**:581–3.

Canale Parola E. Physiology and evolution of spirochetes. *Bacteriol Rev* 1977;**41**:181–204.

Capella-Gutiérrez S, Silla-Martínez JM, Gabaldón T. trimAl: a tool for automated alignment trimming in large-scale phylogenetic analyses. *Bioinformatics* 2009;**25**:1972–3.

Davis NM, Proctor DM, Holmes SP *et al*. Simple statistical identification and removal of contaminant sequences in marker-gene and metagenomics data. *Microbiome* 2018;**6**:1–14.

Domin H, Zurita-Gutiérrez YH, Scotti M *et al*. Predicted bacterial interactions affect *in vivo* microbial colonization dynamics in *Nematostella*. *Front Microbiol* 2018;**9**:1–12.

Drummond AJ, Suchard MA, Xie D *et al*. Bayesian phylogenetics with BEAUti and the BEAST 1.7. *Mol Biol Evol* 2012;**29**:1969–73.

Haegeman B, Hamelin J, Moriarty J *et al*. Robust estimation of microbial diversity in theory and in practice. *ISME J* 2013;**7**:1092–101.

Hand C, Uhlinger KR. The unique, widely distributed, estuarine sea anemone, *Nematostella vectensis* Stephenson: a review, new facts, and questions. *Estuaries* 1994;**17**:501–8.

Har JY, Helbig T, Lim JH *et al*. Microbial diversity and activity in the *Nematostella vectensis* holobiont: insights from 16S rRNA gene sequencing, isolate genomes, and a pilot-scale survey of gene expression. *Front Microbiol* 2015;**6**:818.

Har JY, Introducing the starlet sea anemone *Nematostella vectensis* as a model for investigating microbial mediation of health and disease in hexacorals. Thesis. Massachusetts Institute of Technology, 2009.

Hooper LV, Littman DR, Macpherson AJ. Interactions between the microbiota and the immune system. *Science* 2012;**336**:1268–73.

Høj L, Levy N, Baillie B *et al*. Crown-of-thorns sea star *Acanthaster* cf. *solaris* has tissue-characteristic microbiomes with potential roles in health and reproduction. *Appl Environ Microbiol* 2018;**84**:1–18.

Katoh K, Standley DM. MAFFT multiple sequence alignment software version 7: improvements in performance and usability. *Mol Biol Evol* 2013;**30**:772–80.

Koleff P, Gaston KJ, Lennon JJ. Measuring beta diversity for presence–absence data. *J Anim Ecol* 2003;**72**:367–82.

Lahti L, Shetty S. *Introduction to the Microbiome R Package*. 2018. https://www.bioconductor.org/packages/release/bioc/vignettes/microbiome/inst/doc/vignette.html (15 January 2019, date last accessed).

Lawrence SA, O'Toole R, Taylor MW *et al*. Subcuticular bacteria associated with two common New Zealand echinoderms: characterization using 16S rRNA sequence analysis and fluorescence *in situ* hybridization. *Biol Bull* 2010;**218**:95–104.

Layden MJ, Meyer NP, Pang K *et al*. Expression and phylogenetic analysis of the *zic* gene family in the evolution and development of metazoans. *EvoDevo* 2010;**1**:1–16.

Leach WB, Carrier TJ, Reitzel AM. Diel patterning in the bacterial community associated with the sea anemone *Nematostella vectensis*. *Ecol Evol* 2019;**9**:9935–47.

Liaw A, Wiener M. Classification and regression by randomForest. *R News* 2002;**2**:18–22.

Love MI, Huber W, Anders S. Moderated estimation of fold change and dispersion for RNA-Seq data with DESeq2. *Genome Biol* 2014;**15**:1–21.

McMurdie PJ, Holmes S. phyloseq: an R package for reproducible interactive analysis and graphics of microbiome census data. *PLoS One* 2013;**8**:e61217.

Mortzfeld BM, Urbanski S, Reitzel AM *et al*. Response of bacterial colonization in *Nematostella vectensis* to development, environment and biogeography. *Environ Microbiol* 2016;**18**:1764–81.

Neumann R. Bacterial induction of settlement and metamorphosis in the planula larvae of *Cassiopea andromeda* (Cnidaria: Scyphozoa, Rhizostomeae). *Mar Ecol Prog Ser* 1979;**1**:21–8.

Oksanen J, Blanchet FG, Kindt R *et al*. *vegan: Community Ecology Package*. R package version 1.17-10, 2011. https://cran.r-project.org/web/packages/vegan/index.html (29 November 2020, date last accessed).

Putnam NH, Srivastava M, Hellsten U *et al*. Sea anemone genome reveals ancestral eumetazoan gene repertoire and genomic organization. *Science* 2007;**317**:86–94.

Quast C, Pruesse E, Yilmaz P *et al*. The SILVA ribosomal RNA gene database project: improved data processing and web-based tools. *Nucleic Acids Res* 2013;**41**:590–6.

Quinn TP, Erb I, Richardson MF *et al*. Understanding sequencing data as compositions: an outlook and review. *Bioinformatics* 2018;**34**:2870–8.

Quiroz M, Triadó-Margarit X, Casamayor EO *et al*. Comparison of *Artemia*–bacteria associations in brines, laboratory cultures and the gut environment: a study based on Chilean hypersaline environments. *Extremophiles* 2015;**19**:135–47.

Reese AT, Dunn RR. Drivers of microbiome biodiversity: a review of general rules, feces, and ignorance. *mBio* 2018;**9**:1–14.

Reitzel AM, Ryan JF, Tarrant AM. Establishing a model organism: a report from the first annual *Nematostella* meeting. *BioEssays* 2012;**34**:158–61.

Renfer E, Amon-Hassenzahl A, Steinmetz PRH *et al*. A muscle-specific transgenic reporter line of the sea anemone, *Nematostella vectensis*. *Proc Natl Acad Sci USA* 2010;**107**:104–8.

Robbins SJ, Singleton CM, Chan CX *et al*. A genomic view of the reef-building coral *Porites lutea* and its microbial symbionts. *Nat Microbiol* 2019;**4**:2090–100.

Rosenberg E, Koren O, Reshef L *et al*. The role of microorganisms in coral health, disease and evolution. *Nat Rev Microbiol* 2007;**5**:355–62.

Rossbach S. Tissue-specific microbiomes of the Red Sea giant clam *Tridacna maxima* highlight differential abundance of Endozoicomonadaceae. 2019;**10**:2661.

Rädecker N, Pogoreutz C, Voolstra CR *et al*. Nitrogen cycling in corals: the key to understanding holobiont functioning? *Trends Microbiol* 2015;**23**:490–7.

Stackebrandt E, Chertkov O, Lapidus A *et al*. Genome sequence of the free-living aerobic spirochete *Turneriella parva* type strain (HT), and emendation of the species *Turneriella parva*. *Stand Genomic Sci* 2013;**8**:228–38.

Stamatakis A. RAxML version 8: a tool for phylogenetic analysis and post-analysis of large phylogenies. *Bioinformatics* 2014;**30**:1312–3.

Stefanik DJ, Friedman LE, Finnerty JR. Collecting, rearing, spawning and inducing regeneration of the starlet sea anemone, *Nematostella vectensis*. *Nat Protoc* 2013;**8**:916–23.

Subhash Y, Lee SS. Description of *Oceanispirochaeta sediminicola* gen. nov., sp. nov., an obligately anaerobic bacterium isolated from coastal marine sediments, and reclassification of *Spirochaeta litoralis* as *Oceanispirochaeta litoralis* comb. nov. *Int J Syst Evol Microbiol* 2017;**67**:3403–9.

Sweet MJ, Croquer A, Bythell JC. Bacterial assemblages differ between compartments within the coral holobiont. *Coral Reefs* 2011;**30**:39–52.

Tebben J, Tapiolas DM, Motti CA *et al*. Induction of larval metamorphosis of the coral *Acropora millepora* by tetrabromopyrrole isolated from a *Pseudoalteromonas* bacterium. *PLoS One* 2011;**6**:1–8.

Thompson LR, Sanders JG, McDonald D *et al*. A communal catalogue reveals Earth's multiscale microbial diversity. *Nature* 2017;**551**:457–63.

Vaishnava S, Behrendt CL, Ismail AS *et al*. Paneth cells directly sense gut commensals and maintain homeostasis at the intestinal host–microbial interface. *Proc Natl Acad Sci USA* 2008;**105**:20858–63.

van de Water J, Melkonian R, Junca H *et al*. Spirochaetes dominate the microbial community associated with the red coral *Corallium rubrum* on a broad geographic scale. *Sci Rep* 2016;**6**:1–7.

Weingarten EA, Atkinson CL, Jackson CR. The gut microbiome of freshwater Unionidae mussels is determined by host species and is selectively retained from filtered seston. *PLoS One* 2019;**14**:1–17.

Wessels W, Sprungala S, Watson SA *et al*. The microbiome of the octocoral *Lobophytum pauciflorum*: minor differences between sexes and resilience to short-term stress. *FEMS Microbiol Ecol* 2017;**93**:1–13.

Wolgemuth CW. Flagellar motility of the pathogenic spirochetes. *Semin Cell Dev Biol* 2015;**46**:104–12.

Woznica A, King N. Lessons from simple marine models on the bacterial regulation of eukaryotic development. *Curr Opin Microbiol* 2018;**43**:108–16.

Zenkert C, Takahashi T, Diesner MO *et al*. Morphological and molecular analysis of the *Nematostella vectensis* cnidom. *PLoS One* 2011;**6**:e22725.